SLAC–PUB–7067
December 1995

B Lifetimes and Mixing with the SLD*

John A. Jaros for the SLD Collaboration◊
Stanford Linear Accelerator Center, Stanford University, Stanford, California 94309

The lifetimes of B° and $B^\pm$ mesons have been measured with the SLD detector at the SLC using topological reconstructions of the B mesons. Studies of B_S mixing ,using similar techniques, show that the prospects for measuring B_S mixing with an upgraded vertex detector are good if $x_s \leq 15$.

1. INTRODUCTION

This paper reviews the current status of measurements made with the SLD detector of the charged and neutral B meson lifetimes and discusses prospects for measuring B_s mixing with an upgraded vertex detector. Both analyses rely on topological reconstructions of B meson decays, which are far more efficient than exclusive final state reconstructions. We preface these studies with an overview of the SLD detector, focusing on the performance of the current vertex detector.

2. VERTEX DETECTION WITH THE SLD DETECTOR

The SLC Large Detector (SLD) [1] has recorded the decays of roughly 150K polarized Z° decays produced by the SLAC Linear Collider (SLC) between 1993 and 1995. The elements key to the analyses presented here include the central drift chamber (CDC), which measures charged particle trajectories, the liquid argon calorimeter, which in conjunction with the CDC identifies electrons on the basis of shower energy, and the warm iron calorimeter, which is used to identify penetrating particles as muons. A 0.6T solenoidal magnetic field provides momentum analysis for the CDC.

A CCD pixel vertex detector [2] surrounds the beam pipe just outside the interaction point and—in conjunction with the CDC—provides precise 3-dimensional tracking information. Impact parameter resolution in the plane perpendicular to the e^+e^- beams is $\sigma_{r\varnothing} = 11 \oplus 70/p\sin^{3/2}\theta$ [μm]; it is $\sigma_{rz} = 37 \oplus 70/p\sin^{3/2}\theta$ [μm] in the plane parallel to the incident beams (p is the momentum in GeV/c). The micron-sized transverse beam dimensions provide a small and stable interaction point. Its transverse (longitudinal) position is measured with 7 (50) μm accuracy using sequential hadronic events. The performance of the detector, including even the tails of the impact parameter distributions, is well-modeled by the Monte Carlo simulation.

3. PHYSICS OF B°/B^+ LIFETIMES

Measurements of the lifetimes of the particular B hadron species probe B decay dynamics, normalize the rate determinations from which the CKM element V_{bc} is extracted, and sharpen the description of heavy quark decay topologies. Lifetime differences in the charm sector provided evidence for nonspectator decay

*Work supported in part by Department of Energy contracts: DE–FG02–91ER40676 (BU), DE–FG03–92ER40701 (CIT), DE–FG03–91ER40618 (UCSB), DE–FG03–92ER40689 (UCSC), DE–FG03–93ER40788 (CSU), DE–FG02–91ER40672 (Colorado), DE–FG02–91ER40677 (Illinois), DE–AC03–76SF00098 (LBL), DE–FG02–92ER40715 (Massachusetts), DE–AC02–76ER03069 (MIT), DE–FG06–85ER40224 (Oregon), DE–AC03–76SF00515 (SLAC), DE–FG05–91ER40627 (Tennessee), DE–AC02–76ER00881 (Wisconsin), DE–FG02–92ER40704 (Yale); National Science Foundation grants: PHY–91–13428 (UCSC), PHY–89–21320 (Columbia), PHY–92–04239 (Cincinnati), PHY–88–17930 (Rutgers), PHY–88–19316 (Vanderbilt), PHY–92–03212 (Washington); and by the UK Science and Engineering Research Council (Brunel and RAL); the Istituto Nazionale di Fisica Nucleare of Italy (Bologna, Ferrara, Frascati, Pisa, Padova, Perugia); and by the Japan-US Cooperative Research Project on High Energy Physics (Nagoya, Tohoku).
◊SLD Collboration members and institutions are listed after the references.

Presented at the Production and Decay of Hyperons Charm and Beauty Hadrons, Strasbourg, France, September 5-8, 1995

mechanisms. Beauty decays are thought to follow a pattern analogous to charm, i.e., $\tau(B^+) > \tau(B^\circ) \sim \tau(B_s) > \tau(\Lambda_b)$; but the overall magnitude of lifetime differences, scaling as $1/m_q^2$, is expected to be only 10%. Reference [3] predicts $\tau^+/\tau^\circ = 1.00+0.05\ (f_b/200\ \mathrm{MeV})^2$, where f_b is the B decay constant, indicating a need for experimental precision at the percent level.

In the following, we discuss two separate measurements of the lifetimes of neutral and charged B mesons. The first method (semileptonic) relies on the presence of a high transverse momentum lepton in the event to simplify assumptions about the decay topology. The second method (topological) depends completely on topological identification of B meson charge and decay length. Both methods have been described elsewhere in more detail [4].

4. B°/B^+ LIFETIME–SEMILEPTONIC METHOD

In the semileptonic method, the B decay vertex is taken to be the intersection of the trajectory of a decay lepton and a D meson candidate which is identified topologically. The lepton can be an electron or muon, with at least 2 GeV/c momentum and 400 MeV/c momentum transverse to the nearest jet. The D candidate is made up of tracks which miss the primary interaction point by at least 3.5 standard deviations. A combination of at least two such tracks, which satisfies a three dimensional vertex χ^2 cut, has net charge $|Q_D| \leq 1$, and has invariant mass $m < 1.9\ \mathrm{GeV}/c^2$, constitutes the D. The D vertex must be displaced from the primary by at least four standard errors. The "D" momentum vector approximates the D direction; along with the decay point, it determines the D trajectory. The point of closest approach between the D and lepton trajectories defines the B decay vertex, which is required to be at least 0.8 mm from the IP. The invariant mass of all the tracks in the B must exceed $1.4\ \mathrm{GeV}/c^2$, the net charge $|Q_B| \leq 1$, and the distance between the B and D vertices must exceed 200 μm. As a final step, other tracks in the event are attached to either the B or the D decay vertices if the resulting vertex χ^2's are sufficiently low.

Three topologies are allowed for neutral B mesons: a single prong (the lepton) at the B vertex along with a three prong "D"; two prongs at the B vertex (the lepton and a transition pion from a D*) along with either two or four prongs at the "D" vertex. Charged B mesons decay predominantly to D° mesons, so the D vertex is required to be neutral and contain two or four prongs. The B vertex is required to be a single prong for charged B's.

The algorithm selects 428 neutral and 549 charged decays from the 150 K hadronic Z° decay sample. Monte Carlo studies give the B composition of the neutral (charged) sample as 15.8% (70.1%) B_u, 65.4% (18.4%) B_d, 13.6% (4.1%) B_s, and 4.1% (2.3%) B baryon. Roughly 1.3% (5.1%) of the neutral (charged) sample is non-B background. As shown in Fig. 1, the charge multiplicities observed at the B and D vertices agree with Monte Carlo expectation, which substantiates the charge assignment. The beam polarization at the SLC provides a second check of the charge assignment. Polarized Z decays give rise to a left-right, forward-backward asymmetry [5]. Figure 2 shows this asymmetry for the charged and neutral samples as a function of $\cos\theta_b$, where θ_b is the production angle of the b quark with respect to the direction of the electron beam. Lepton charge identifies the quark as b or $\bar{b}$. The charged B sample has the expected asymmetry. The neutral B sample is also consistent with

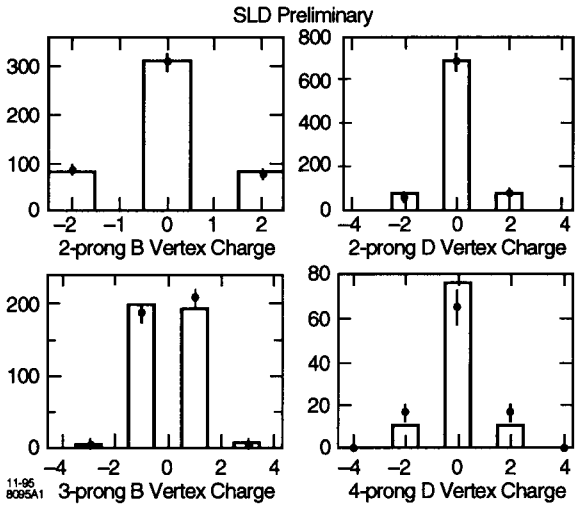

Figure 1. Measured distribution of vertex charges (data points) compared to Monte Carlo simulation (histogram) for the semileptonic analysis.

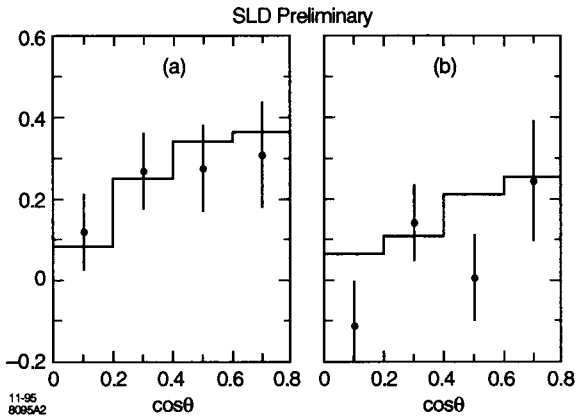

Figure 2. The left-right forward-backward asymmetry for (a) charged and (b) neutral decays. Data are shown as points and the Monte Carlo as histograms.

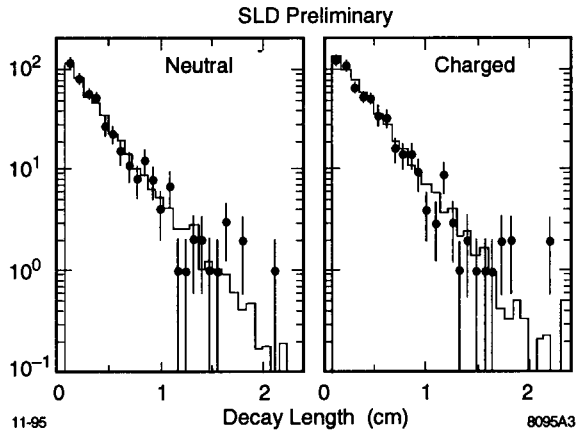

Figure 3. Decay length distribution for the neutral and charged B meson decays in the semileptonic analysis. The Monte Carlo simulation is shown with the histogram.

expectation, and is diluted by B mixing effects, confirming the charge assignment.

The measured decay length distributions are shown in Fig. 3 for both samples. The Monte Carlo is used to generate a fitting function for these distributions, incorporating the spectrum of B energies expected from fragmentation effects. A binned maximum likelihood fit to both distributions extracts the lifetime ratio and each of the separate lifetimes. Systematic errors are dominated by systematics of the fitting procedure, B physics modeling (especially the fragmentation function) and tracking efficiencies. Preliminary results are as follows:

$$\tau_{B^\circ} = 1.60^{+0.15}_{-0.14} \pm 0.10 \text{ ps}$$

$$\tau_{B^\pm} = 1.49^{+0.11}_{-0.10} \pm 0.05 \text{ ps}$$

$$\tau_{B^+} / \tau_{B^\circ} = 0.94^{+0.14}_{-0.12} \pm 0.07 \text{ ps} .$$

5. B°/B^+ LIFETIME-TOPOLOGICAL METHOD

The second method used to measure the charged and neutral B meson lifetimes relies exclusively on topological vertexing. A sample of $b\bar{b}$ events is selected with an impact parameter tag. Strict quality cuts are imposed on the tracks. Secondary vertices are identified [6] as regions of high track overlap probability, where tracks are represented as 3-dimensional probability tubes, their transverse size reflecting impact parameter errors. Individual vertices are clustered together if they are not clearly resolvable, and tracks are associated with the clusters on the basis of a χ^2 test.

Two-thirds of the tagged events have at least one secondary vertex reconstructed. The secondary vertex farthest from the IP is selected in events having more than one vertex in an event hemisphere. Additional tracks are associated with the secondary if they pass within 1 mm of the line joining the IP to the secondary, and if the distance between the IP and their point of closest approach to the decay line is at least 30% of the distance to the secondary. The invariant mass of all the tracks associated with the secondary must exceed 2 GeV/c^2 in order to remove charm contamination, and the decay length of the resultant vertex must exceed 1 mm. Additional tracks, with less stringent quality cuts, are included in the secondary vertex for the charge determination. The algorithm reconstructs 3382 neutral and 5303 charged decays, which have charge $|Q| \geq 1$. Monte Carlo studies show that 99.3% of the selected events are in fact $b\bar{b}$. The neutral (charged) sample consists of 22.2% (56.2%) B_u, 55.5% (29.8%) B_d, 15.3% (8.2%) B_S, and 6.3% (4.8%) B baryon.

The observed charge distribution shown in Fig. 4 is in excellent agreement with Monte Carlo simulation. A second check on the charge assignment is the observation of the forward-backward asymmetry for the charged B meson sample. In this sample, the charge of the meson is a measure of the quark charge. Consequently,

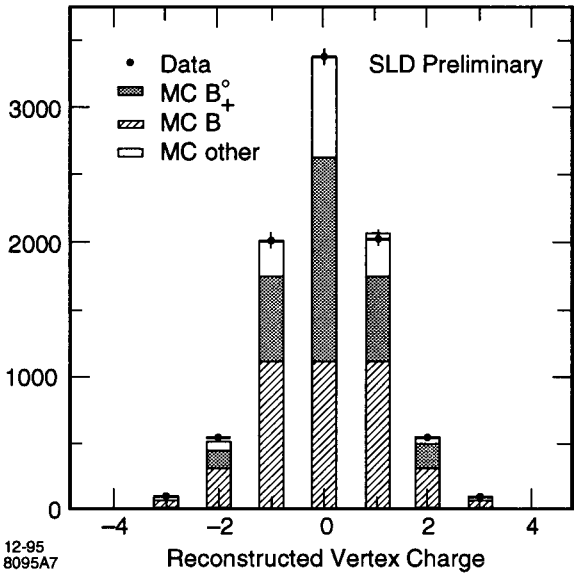

Figure 4. Distribution of charges reconstructed in the topological analysis. Data are shown as points and the Monte Carlo simulation as the histogram.

as shown in Fig. 5, the observed angular distribution shows a distinct asymmetry. The agreement between the data and Monte Carlo simulation is good for both the 1993 ($\langle P_e \rangle$ = 63.0±1.1%) and 1994-5 ($\langle P_e \rangle$ = 77.3±0.6%) running, confirming that the charge assignment is correctly modeled.

The observed decay lengths for the neutral and charged samples are shown in Fig. 6. The

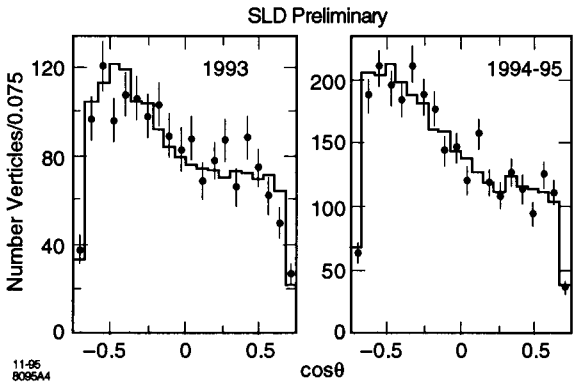

Figure 5. Measured (data points) and predicted (histogram) asymmetries for charged B decays. The measured B production angle is signed with the product of the B meson charge and incident electron helicity.

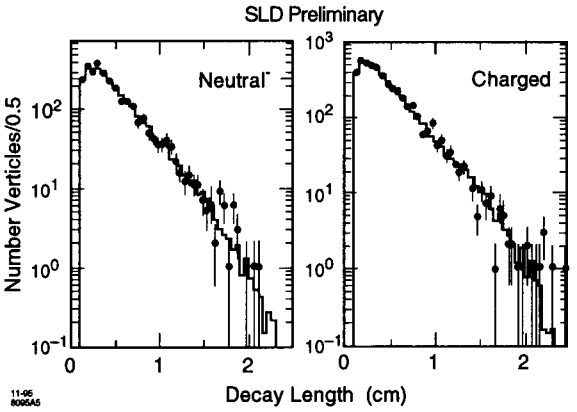

Figure 6. Decay length distribution for charged and neutral B meson decays in the topological analysis. The histogram is the Monte Carlo prediction corresponding to the best fit.

two-parameter fit proceeds as in the semileptonic analysis, with the two distributions being fit simultaneously. The fitting function is again derived from the Monte Carlo and thus includes effects from B energy spread and the fact that tracks from both secondary B and tertiary D decays can be included in the decay length determination. The systematic errors are dominated by uncertainties in the tracking efficiency, fit systematics, and B fragmentation and decay multiplicities. Preliminary results are as follows:

$$\tau_{B^\circ} = 1.55 \pm 0.07 \pm 0.12 \text{ ps}$$

$$\tau_{B^\pm} = 1.67 \pm 0.06 \pm 0.09 \text{ ps}$$

$$\tau_{B^+} / \tau_{B^\circ} = 1.08^{+0.09}_{-0.08} \pm 0.10 \text{ ps} .$$

These results are consistent with those from the semileptonic analysis presented above and those from other experiments. They are also consistent with the theoretical expectation that the charged and neutral B mesons have roughly equal lifetimes. The errors in this analysis are competitive with those from experiments with much larger data sets, illustrating the statistical power of topological vertexing, and promising much reduced errors in the future.

6. MOTIVES FOR MEASURING B_S MIXING

B_S and B_d mixing, taken together, determine the least well known side of the unitarity triangle, Vtd/Vbc, with only 10% theoretical uncertainty [7]. This comes about because uncertainties in the B meson masses, bag factors, and decay constants largely cancel when one takes the ratio between the oscillation frequencies for B_S and B_d mixing. This accuracy may be sufficient to establish whether or not the CKM phase is nonzero, or equivalently, whether CKM mixing is a source of CP violation. In fact, the measurement of B_S mixing could well be the first test of this standard model source of CP violation. If CP violation in the K system is the result of CKM mixing, the mixing parameter is expected to lie in the range $6 < x_s < 33$ [7]. This corresponds to rapid B_S oscillations (on the scale of the B lifetime), and requires proper time resolution in the 3–10% range to be seen. Successful observation of B_S mixing is likely to require excellent decay length resolution and good boost resolution.

7. MEASURING B_S MIXING WITH THE SLD

Two features of the SLC enhance our ability to measure B_S mixing with the SLD. The polarization of the electron beam permits control of the Z° polarization. Since the angular distribution of b quarks is strongly asymmetric, and depends on the known sign of the polarization, the initial b quark charge is tagged by the production angle:

$$\frac{d\sigma}{d\cos\theta_b} = \left(1 - A_e P_e\right)\left(1 + \cos^2\theta_B\right) + 2A_b\left(A_e - P_e\right)\cos\theta_B \ .$$

Note that a polarization tag is 100% efficient. With beam polarizations near 80%, it has an analyzing power, averaged over the useful solid angle, of 0.5. The tiny, well-defined interaction point, and the small beam pipe radius at the SLC permit very high resolution vertex detection, which is needed to probe high x_s.

An upgraded CCD vertex detector [8] will be installed prior to the January 1996 SLD run. The new detector is based on very large area (1.5×8 cm^2) CCDs and will provide improved solid angle coverage ($\Delta\Omega$=.75→0.90), overlapping three-layer coverage, thinner layers (x/x_0=1.2%→0.4%/layer), and an increased lever arm, all of which result in significantly improved resolutions: $\sigma_{r\phi} = 7 + 37/p \sin^{3/2}\theta$ [μm]; $\sigma_{rz} = 14 \oplus 37/p \sin^{3/2}\theta$ [μm]. The improved resolution increases sensitivity to high x_s and boosts event selection efficiencies. The larger solid angle improves acceptance and results in increased analyzing power.

To measure B_S mixing requires knowledge of the initial quark charge, which is tagged by polarization and jet-charge; the final quark charge, which is tagged by lepton charge; and the B decay length and the B energy. The decay length is determined with the semileptonic method described above. The signal for B_S mixing is a high frequency oscillatory component of the proper time distribution, which is visible once the mixed and unmixed samples have been separated.

8. THE x_s REACH

Studies [9] of the x_s reach of the upgraded detector have used full Monte Carlo to evaluate vertexing efficiencies (41%), decay length resolution (200 μm), and boost resolution (10%) and acceptance. The present studies assume a 500 kZ sample with the upgraded vertex detector, 80% beam polarization, and 12% B_s fraction. Using these parameters as input, a fast Monte Carlo is used to generate an ensemble of experiments, the simulated data of which are fit with a maximum likelihood technique. Besides finding the optimum value of x_s, the fit assigns a significance by determining the difference in log likelihood between the optimum x_s and as-

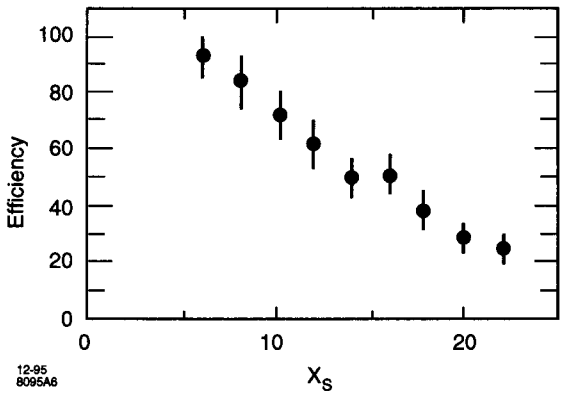

Figure 7. Efficiency to observe a B_s mixing signal with a significance ≥ 2.5 as a function of the oscillation frequency, x_s.

significance by determining the difference in log likelihood between the optimum x_s and asymptotically high x_s. The significance must be reasonably high, or a false minimum may be detected. The experiment's reach for a significance cut of 2.5 (and corresponding fake rate of 5%) is shown in Fig. 7, which plots the efficiency for detecting a result at or above the significance cut as a function of x_s. The experiment has a reasonable chance to see B_s mixing up to x_s of 15 or so.

Several improvements should extend SLD's reach beyond the baseline established above. The vertexing efficiency can likely be improved, as can the sample purity (by requiring neutrals only or kaon tagging). The most significant improvements may come from topological tags of final quark charge, made possible by identifying charged D's in the decay products.

9. CONCLUSIONS

The charged and neutral B meson lifetimes, and their ratio, have been measured with the SLD detector using new techniques which rely heavily on topological vertexing. The installation of an improved CCD vertex detector and an anticipated quadrupling of the size of the data set will yield lifetime measurements with sufficient accuracies to test theoretical expectations. Using the new vertex detector and polarization tagging, the SLD will be sensitive to B_s mixing for values of the oscillation parameter $x_s \leq 15$.

REFERENCES

1. G. Agnew et al., SLD Design Report, SLAC–0273 (1984).
2. G. Agnew et al., SLAC–PUB–5906.
3. I. I. Bigi, UND–HEP–95–BIG–06 (1995).
4. SLD Collaboration, SLAC–PUB–95–6972 (1995). Contributed to the International Symposium on Lepton-Photon Interactions, Beijing, China, 1995.
5. K. Abe et al., Phys. Rev. Lett. **74**, 2895 (1995).
6. D. Jackson, SLD Physics Note 37.
7. A. Ali, D. London, Z. Phys. **C65**, 431 (1995).
8. SLD Vertex Detector Upgrade Group, SLAC-PUB-95-6950 (1995).
9. G. Zapalac, SLD Physics Note 42.

The SLD Collboration

K. Abe,[29] I. Abt,[14] C.J. Ahn,[26] T. Akagi,[27] N.J. Allen,[4] W.W. Ash,[27,†]
D. Aston,[27] K.G. Baird,[25] C. Baltay,[33] H.R. Band,[32] M.B. Barakat,[33]
G. Baranko,[10] O. Bardon,[16] T. Barklow,[27] A.O. Bazarko,[11] R. Ben-David,[33]
A.C. Benvenuti,[2] T. Bienz,[27] G.M. Bilei,[22] D. Bisello,[21] G. Blaylock,[7]
J.R. Bogart,[27] T. Bolton,[11] G.R. Bower,[27] J.E. Brau,[20] M. Breidenbach,[27]
W.M. Bugg,[28] D. Burke,[27] T.H. Burnett,[31] P.N. Burrows,[16] W. Busza,[16]
A. Calcaterra,[13] D.O. Caldwell,[6] D. Calloway,[27] B. Camanzi,[12] M. Carpinelli,[23]
R. Cassell,[27] R. Castaldi,[23][a] A. Castro,[21] M. Cavalli-Sforza,[7] E. Church,[31]
H.O. Cohn,[28] J.A. Coller,[3] V. Cook,[31] R. Cotton,[4] R.F. Cowan,[16] D.G. Coyne,[7]
A. D'Oliveira,[8] C.J.S. Damerell,[24] M. Daoudi,[27] R. De Sangro,[13] P. De Simone,[13]
R. Dell'Orso,[23] M. Dima,[9] P.Y.C. Du,[28] R. Dubois,[27] B.I. Eisenstein,[14] R. Elia,[27]
E. Etzion,[4] D. Falciai,[22] M.J. Fero,[16] R. Frey,[20] K. Furuno,[20] T. Gillman,[24]
G. Gladding,[14] S. Gonzalez,[16] G.D. Hallewell,[27] E.L. Hart,[28] Y. Hasegawa,[29]
S. Hedges,[4] S.S. Hertzbach,[17] M.D. Hildreth,[27] J. Huber,[20] M.E. Huffer,[27]
E.W. Hughes,[27] H. Hwang,[20] Y. Iwasaki,[29] D.J. Jackson,[24] P. Jacques,[25]
J. Jaros,[27] A.S. Johnson,[3] J.R. Johnson,[32] R.A. Johnson,[8] T. Junk,[27]
R. Kajikawa,[19] M. Kalelkar,[25] H. J. Kang,[26] I. Karliner,[14] H. Kawahara,[27]
H.W. Kendall,[16] Y. Kim,[26] M.E. King,[27] R. King,[27] R.R. Kofler,[17]
N.M. Krishna,[10] R.S. Kroeger,[18] J.F. Labs,[27] M. Langston,[20] A. Lath,[16]
J.A. Lauber,[10] D.W.G. Leith,[27] M.X. Liu,[33] X. Liu,[7] M. Loreti,[21] A. Lu,[6]
H.L. Lynch,[27] J. Ma,[31] G. Mancinelli,[22] S. Manly,[33] G. Mantovani,[22]
T.W. Markiewicz,[27] T. Maruyama,[27] R. Massetti,[22] H. Masuda,[27] E. Mazzucato,[12]
A.K. McKemey,[4] B.T. Meadows,[8] R. Messner,[27] P.M. Mockett,[31] K.C. Moffeit,[27]
B. Mours,[27] G. Müller,[27] D. Muller,[27] T. Nagamine,[27] U. Nauenberg,[10] H. Neal,[27]
M. Nussbaum,[8] Y. Ohnishi,[19] L.S. Osborne,[16] R.S. Panvini,[30] H. Park,[20]
T.J. Pavel,[27] I. Peruzzi,[13][b] M. Piccolo,[13] L. Piemontese,[12] E. Pieroni,[23]
K.T. Pitts,[20] R.J. Plano,[25] R. Prepost,[32] C.Y. Prescott,[27] G.D. Punkar,[27]
J. Quigley,[16] B.N. Ratcliff,[27] T.W. Reeves,[30] J. Reidy,[18] P.E. Rensing,[27]
L.S. Rochester,[27] J.E. Rothberg,[31] P.C. Rowson,[11] J.J. Russell,[27] O.H. Saxton,[27]
S.F. Schaffner,[27] T. Schalk,[7] R.H. Schindler,[27] U. Schneekloth,[16] B.A. Schumm,[15]
A. Seiden,[7] S. Sen,[33] V.V. Serbo,[32] M.H. Shaevitz,[11] J.T. Shank,[3] G. Shapiro,[15]
S.L. Shapiro,[27] D.J. Sherden,[27] K.D. Shmakov,[28] C. Simopoulos,[27] N.B. Sinev,[20]
S.R. Smith,[27] J.A. Snyder,[33] P. Stamer,[25] H. Steiner,[15] R. Steiner,[1]
M.G. Strauss,[17] D. Su,[27] F. Suekane,[29] A. Sugiyama,[19] S. Suzuki,[19] M. Swartz,[27]
A. Szumilo,[31] T. Takahashi,[27] F.E. Taylor,[16] E. Torrence,[16] J.D. Turk,[33]
T. Usher,[27] J. Va'vra,[27] C. Vannini,[23] E. Vella,[27] J.P. Venuti,[30] R. Verdier,[16]
P.G. Verdini,[23] S.R. Wagner,[27] A.P. Waite,[27] S.J. Watts,[4] A.W. Weidemann,[28]
E.R. Weiss,[31] J.S. Whitaker,[3] S.L. White,[28] F.J. Wickens,[24] D.A. Williams,[7]
D.C. Williams,[16] S.H. Williams,[27] S. Willocq,[33] R.J. Wilson,[9] W.J. Wisniewski,[5]
M. Woods,[27] G.B. Word,[25] J. Wyss,[21] R.K. Yamamoto,[16] J.M. Yamartino,[16]
X. Yang,[20] S.J. Yellin,[6] C.C. Young,[27] H. Yuta,[29] G. Zapalac,[32] R.W. Zdarko,[27]
C. Zeitlin,[20] Z. Zhang,[16] and J. Zhou,[20]

[1]Adelphi University, Garden City, New York 11530
[2]INFN Sezione di Bologna, I-40126 Bologna, Italy
[3]Boston University, Boston, Massachusetts 02215
[4]Brunel University, Uxbridge, Middlesex UB8 3PH, United Kingdom
[5]California Institute of Technology, Pasadena, California 91125
[6]University of California at Santa Barbara, Santa Barbara, California 93106
[7]University of California at Santa Cruz, Santa Cruz, California 95064
[8]University of Cincinnati, Cincinnati, Ohio 45221
[9]Colorado State University, Fort Collins, Colorado 80523
[10]University of Colorado, Boulder, Colorado 80309
[11]Columbia University, New York, New York 10027
[12]INFN Sezione di Ferrara and Università di Ferrara, I-44100 Ferrara, Italy
[13]INFN Lab. Nazionali di Frascati, I-00044 Frascati, Italy
[14]University of Illinois, Urbana, Illinois 61801
[15]Lawrence Berkeley Laboratory, University of California, Berkeley, California 94720
[16]Massachusetts Institute of Technology, Cambridge, Massachusetts 02139
[17]University of Massachusetts, Amherst, Massachusetts 01003
[18]University of Mississippi, University, Mississippi 38677
[19]Nagoya University, Chikusa-ku, Nagoya 464 Japan
[20]University of Oregon, Eugene, Oregon 97403
[21]INFN Sezione di Padova and Università di Padova, I-35100 Padova, Italy
[22]INFN Sezione di Perugia and Università di Perugia, I-06100 Perugia, Italy
[23]INFN Sezione di Pisa and Università di Pisa, I-56100 Pisa, Italy
[25]Rutgers University, Piscataway, New Jersey 08855
[24]Rutherford Appleton Laboratory, Chilton, Didcot, Oxon OX11 0QX United Kingdom
[26]Sogang University, Seoul, Korea
[27]Stanford Linear Accelerator Center, Stanford University, Stanford, California 94309
[28]University of Tennessee, Knoxville, Tennessee 37996
[29]Tohoku University, Sendai 980 Japan
[30]Vanderbilt University, Nashville, Tennessee 37235
[31]University of Washington, Seattle, Washington 98195
[32]University of Wisconsin, Madison, Wisconsin 53706
[33]Yale University, New Haven, Connecticut 06511
[†]Deceased
[a]Also at the Università di Genova
[b]Also at the Università di Perugia